

## ■ Rationale for Mid-Cycle Time

The observations proposed here and the experiment they enable, a test of the Ly $\alpha$  line reconstruction routines, will be of immediate use to multiple groups and projects. They will contribute to the analysis of many past HST observing programs, and inform the design of future Ly $\alpha$  observations in the next cycle. The analysis of the COS data leading to the design of this experiment was not completed until after the last proposal deadline.

## ■ Science Justification

The H I Lyman  $\alpha$  (Ly $\alpha$ ) line at 1215.67 Å is a paradox of stellar observational astronomy: Vitally important for the study of stellar atmospheres and their effects on orbiting exoplanets, contributing as it does a large fraction of the ultraviolet flux ( $\approx 30\text{--}70$  per cent, France et al. 2013) of low mass stars; but extremely difficult to observe, occulted almost entirely by a combination of absorption by interstellar hydrogen and airglow emission from the Earth’s atmosphere. Nevertheless, observations of the Ly $\alpha$  line are the focus of a large number of HST observing programs, returning data from dozens of stars to date. These programs have been used to, for example, measure stellar winds (Wood, 2018), estimate the extreme ultraviolet flux of stars (Linsky et al., 2014), and model the atmospheres of the TRAPPIST-1 planets (Bourrier et al., 2017; Wunderlich et al., 2020). Improving the accuracy of Ly $\alpha$  reconstructions, the chief goal of this proposal, is particularly important for accurately modeling chemistry in exoplanet atmospheres. Small changes of  $\sim 20$  per cent in the reconstructed Ly $\alpha$  flux can propagate to  $\sim 30$  per cent changes in the O<sub>2</sub> and O<sub>3</sub> column depths in Earth-like planets orbiting M dwarfs (Segura et al., 2007). In mini-Neptune atmospheres, Ly $\alpha$  is the dominant driver of photochemistry in the atmospheric layers most likely to be probed by future direct observations (Miguel et al., 2015).

Stellar Ly $\alpha$  observations rely on the fact that the Ly $\alpha$  lines of their targets are broad enough that the wings of the line are detectable to one or both sides of the regions occluded by ISM absorption and/or airglow. The full profile and strength of the Ly $\alpha$  line can then be reconstructed from the wings. Multiple methods have been developed for the reconstruction, such as using metal lines to characterise and thus remove the ISM (Wood et al., 2005) and/or fitting model line profiles to the wings (Bourrier et al., 2015; Youngblood et al., 2016), with broad agreement between techniques and recipes. However, statistical uncertainties in the reconstructions, which range from 5 per cent to 100 per cent depending on the data quality (Wood et al., 2005; Youngblood et al., 2016), are dominated by degeneracies between the ISM absorbers and intrinsic stellar profile as well as our incomplete knowledge of the intrinsic Ly $\alpha$  profile shape for essentially all stars.

Testing the absolute accuracy of these reconstructions is challenging, as the ground truth of occulted Ly $\alpha$  profiles cannot be obtained. In some cases the Ly $\alpha$  line can be fully observed at stars with sufficiently high radial velocities to shift the line out of the airglow and the deepest ISM absorption, the best example being Kapteyn’s star at  $245\text{ km s}^{-1}$  (Guinan et al., 2016; Schneider et al., 2019). Unfortunately they cannot be used as tests for the reconstruction techniques, as they cannot also be observed with the line occulted. What

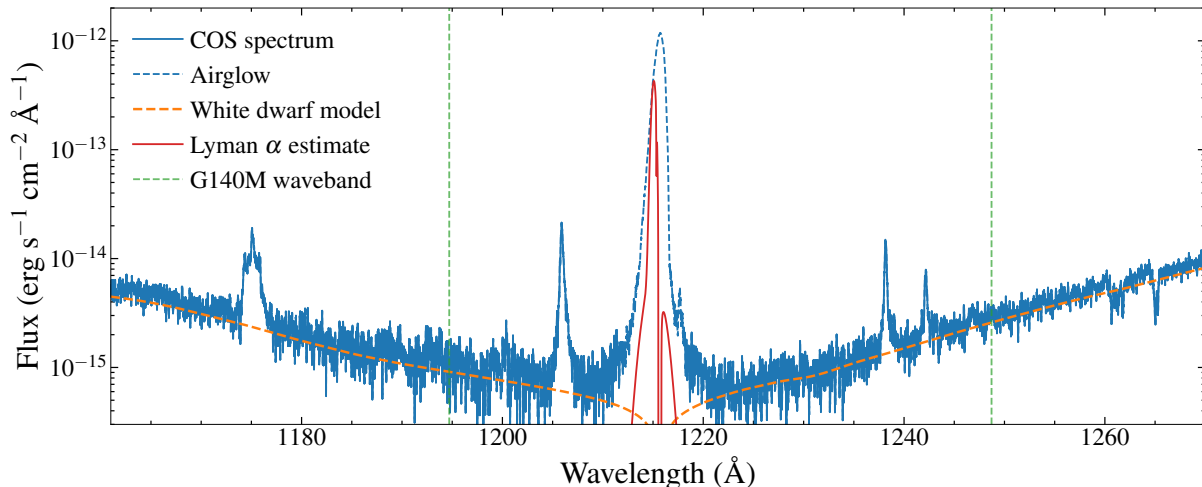


Figure 1: Segment A of the COS G130L spectrum of EG UMa. The spectrum is dominated by multiple emission lines from the M dwarf. The predicted strong Lyman  $\alpha$  line is entirely lost to airglow in the COS observation, but would be easily detectable at multiple velocities with STIS.

is required is a star where the radial velocity changes by many 10s of  $\text{km s}^{-1}$  over time, allowing observations to be taken at low velocities when the Ly $\alpha$  line is occulted, and the reconstruction based on that data compared with unocculted, high-velocity Ly $\alpha$  observations. Such conditions exist in close binaries. We have identified perhaps the only system where this experiment is possible, and request STIS time to obtain the observations necessary to validate the vital Ly $\alpha$  reconstructions.

EG UMa is a close binary comprised of a M4 type M dwarf in a 16 hour orbit of a white dwarf (Lanning, 1982; Bleach et al., 2000). The white dwarf is unusually cool for such systems with an effective temperature of only  $\approx 13000$  K (Sion et al., 1984), such that the ultraviolet emission is not completely dominated by the white dwarf, containing detectable contribution from the M dwarf. Figure 1 shows the A segment of a COS G130M spectrum of the system. Strong emission lines from ions including C III, Si II and N V in the M dwarf atmosphere with peak fluxes several times greater than the white dwarf flux are readily detected. We found no significant change in the line strengths over the four subspectra taken during the COS observation, indicating that the star was not flaring. Furthermore, the white dwarf spectrum is very well described by a Koester (2010) model atmosphere fit (orange line in Figure 1) and can be subtracted, leaving an M dwarf emission line spectrum analogous to what would be observed at any given single M dwarf. The short orbital period provides the large range of radial velocities that would allow the system to be observed at multiple levels of Ly $\alpha$  occultation, allowing a comprehensive test of Ly $\alpha$  reconstruction routines. The peak radial velocity (combining the orbital motion of the M dwarf and net velocity of the system relative to Earth) is  $\approx -160 \text{ km s}^{-1}$ , at which point the peak and  $\gtrsim 90$  per cent of

the wings of the Ly $\alpha$  profile will be well clear of the airglow occultation and the deepest ISM absorption (Figure 3, right panel). The shape of the Ly $\alpha$  line core (particularly its self reversal) diagnoses the opacity of the chromosphere, which may be related to magnetic field strength as evidenced by spatially resolved Ly $\alpha$  spectra of the Sun (Fontenla et al., 1988; Curdt et al., 2001). An observation at  $-160 \text{ km s}^{-1}$  would add to the small number of stars ( $\sim 5$ ) for which we can directly probe the intrinsic shape of the Ly $\alpha$  line core.

The wide, slitless aperture of COS means that the contribution from airglow at Ly $\alpha$  completely obscures the emission from the star, as Figure 1 clearly shows. We will therefore observe with STIS, using the G140M grating at a central wavelength of  $1222 \text{ \AA}$ , the setup used for the majority of Ly $\alpha$  stellar observations. As detailed in the description of the observations, we constructed a predicted spectrum based on the COS data and used that to confirm that STIS has the required sensitivity for these observations.

Radial velocity measurements of EG UMa by Bleach et al. (2000) provided a precise determination of the orbital period and ephemeris, allowing for accurately phase-resolved observations. The observing strategy is outlined in Figure 2, showing the radial velocity curve of the M dwarf and the ideal observing times. Note however that around the peaks the radial velocity changes by only  $\sim 10 \text{ km s}^{-1}$  over several hours, so the phase timing requirements for the program can be quite forgiving.

Two orbits (observations 1 and 3 in Figure 2) will observe the system when the net radial velocity of the M dwarf is near zero (within a small, acceptable range produced by the combination of the systemic velocity and the Earth’s heliocentric velocity), providing the maximum occultation of the Ly $\alpha$  line. Observing for two orbits will increase the S/N of the Ly $\alpha$  wings to lower the statistical error on the line reconstruction process. We will also a spectrum at the peak redshift at  $\approx -90 \text{ km s}^{-1}$  (observation 4 in Figure 2), providing a partially occulted line similar to those observed at many stars. Panels one and three of Figure 3 show our simulated G140M spectra at these phases, with the noise level from an exposure time of 2000 s calculated using the STIS Exposure Time Calculator. Finally, we will observe at the peak blueshift with a radial velocity of  $\approx -160 \text{ km s}^{-1}$  (Figure 3, middle panel), providing the almost entirely unocculted Ly $\alpha$  profile against which we can test the accuracy of our reconstructions to both the fully and partially obscured lines.

We are therefore testing the reconstructions in two different ways: How do the reconstructions compare to the true Ly $\alpha$  profile; and how do two reconstructions of the same star at different levels of occultation compare? Combined, these experiments will be a comprehensive diagnostic of any systematic uncertainties present in the reconstruction recipes, and will provide the ground truth data required to correct such uncertainties. Our observing strategy also accounts for potential interference from flares and/or heating from the companion, as detailed further in the description of the observations.

In conclusion, we have shown that the observations and experiment design proposed here will allow us to successfully validate the Ly $\alpha$  reconstruction methods. Given the huge amount of HST time invested in Ly $\alpha$  observations, this experiment and the data behind it represent a vital resource for interpreting Ly $\alpha$  observations and, by extension, understanding the atmospheres of stars and exoplanets.

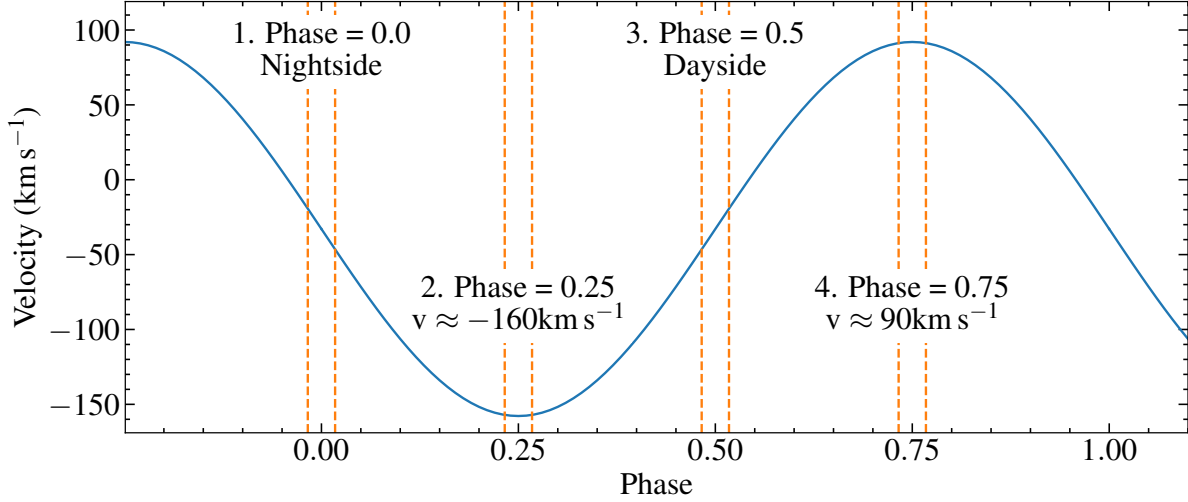


Figure 2: Radial velocity phase curve of the M dwarf showing the planned observation epochs. The dashed lines show the phase coverage of the approximate time-on-target achievable within a single HST orbit. The long period means that the velocity does not change by more than a few  $\text{km s}^{-1}$  per HST orbit at the peaks, giving considerable flexibility when scheduling the observations.

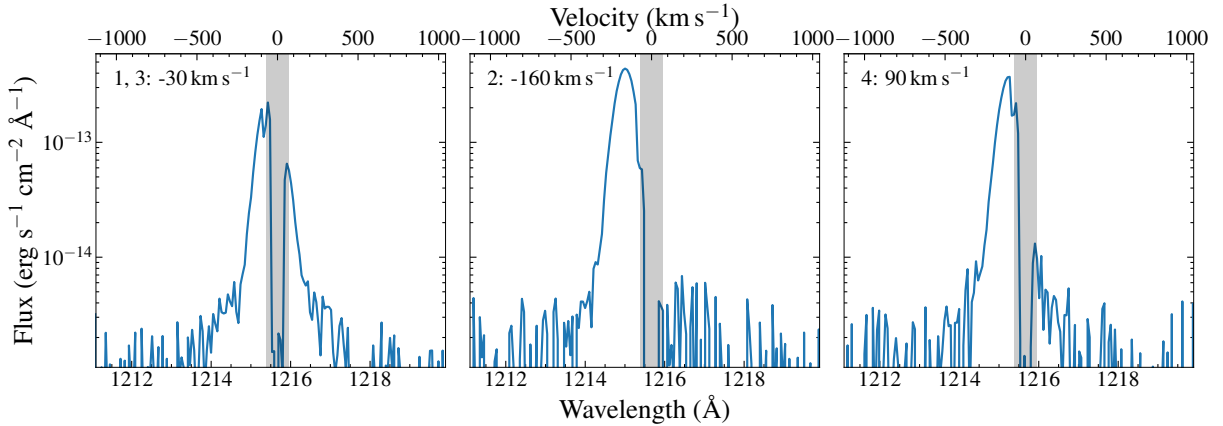


Figure 3: Simulated Lyman  $\alpha$  lines at each of the observed epochs in Figure 2. The grey bar shows the approximate range lost to airglow. We will reconstruct the Lyman  $\alpha$  line based on epoch 1, 3, and 4 (left and right panels), and compare the accuracy of our reconstruction with the spectrum at epoch 2 (middle panel), where the majority of the line profile is clear of the airglow and deep ISM absorption.

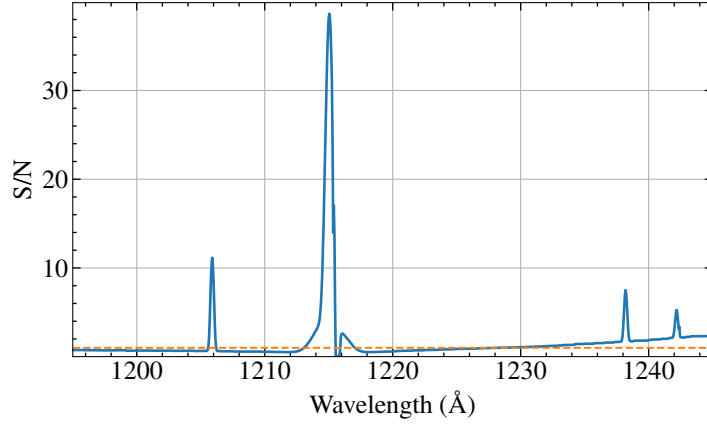


Figure 4: Signal to noise prediction for a single orbit produced using our predicted spectrum and the STIS ETC. The spectrum was calculated at a velocity of  $150 \text{ km s}^{-1}$ . The orange dashed line shows  $S/N=1$ . The  $\text{Ly}\alpha$  line (if unocculted) and other emission lines are clearly observed in a single orbit. However the  $S/N$  of the  $\text{Ly}\alpha$  wings is lower, hence the request for two orbits at phases with low velocity where some or all of the peak is obscured.

## References

- Curdt, W., Brekke, P., Feldman, U., et al. 2001, *A&A*, 375, 591
- Wood, B. E., Redfield, S., Linsky, J. L., et al. 2005, *ApJS*, 159, 118
- Bourrier, V., Ehrenreich, D., & Lecavelier des Etangs, A. 2015, , 582, A65
- Wood, B. E. 2018, *Journal of Physics Conference Series*, 1100, 012028
- Linsky, J. L., Fontenla, J., & France, K. 2014, *ApJ*, 780, 61
- Wunderlich, F., Scheucher, M., Godolt, M., et al. 2020, *arXiv:2006.11349*
- Bourrier, V., de Wit, J., Bolmont, E., et al. 2017, , 154, 121
- Fontenla, J., Reichmann, E. J., Tandberg-Hanssen, E. 1988, *ApJ*, 329, 464
- France, K., Froning, C. S., Linsky, J. L., et al. 2013, *ApJ*, 763, 149
- Schneider, A. C., Shkolnik, E. L., Barman, T. S., et al. 2019, *ApJ*, 886, 19
- Bleach, J. N., Wood, J. H., Catalán, M. S., et al. 2000, , 312, 70
- Segura, A., Meadows, V. S., Kasting, J. F., Crisp, D., Cohen, M. 2007, *A&A*, 472, 665
- Sion, E. M., Wesemael, F., & Guinan, E. F. 1984, *ApJ*, 279, 758
- Lanning, H. H. 1982, *ApJ*, 253, 752
- Miguel, Y., Kaltenegger, L., Linsky, J. L., Rugheimer, S. 2015, , 446, 345
- Redfield, S. & Linsky, J. L. 2008, *ApJ*, 673, 283
- Koester, D. 2010, , 81, 921
- Froning, C. S., Kowalski, A., France, K., et al. 2019, , 871, L26
- Guinan, E. F., Engle, S. G., & Durbin, A. 2016, *ApJ*, 821, 81
- Youngblood, A., France, K., Loyd, R. O. P., et al. 2016, *ApJ*, 824, 101

## ■ Description of the Observations

We will observe the binary EG UMa for four orbits, phase resolved as described in the scheduling requirements. The observations will use STIS in spectroscopic mode with the G140M grating and a cenwave of 1222Å.

We constructed a simulated spectrum based on the white dwarf model, fits to the observed emission lines in the COS spectrum, an approximate Ly $\alpha$  profile estimated from the strength of those emission lines, and an ISM profile estimated from the Redfield & Linsky (2008) velocity calculator and a 2D interpolation of available H I density measurements to the sightline of EG UMa, all interpolated onto the wavelength grid of an archival STIS G140M spectrum. The ISM profile was calculated with velocity centroid of  $1.45 \text{ km s}^{-1}$ , Doppler  $b = 11.5 \text{ km s}^{-1}$  and  $\log N(\text{HI}) = 17.94$ .

Using the model spectrum as an input for the STIS ETC we estimate achieving a peak S/N of  $\approx 40$  for the Ly $\alpha$  line in a single orbit, sufficient for the aims of this program (Figure 4). Emission lines of Si III and N V are also detected with  $S/N \approx 10$ , which we can use to track for flares and (unlikely) heating effects from the companion.

The target has already been cleared for bright object protection for the previous COS observation.

Our observing strategy accounts for two potential concerns. Firstly, the Mdwarf is active, with multiple flares in the TESS light curve of EG UMa. We calculate a flare duty cycle of  $\approx 5$  per cent, so the chances of the star flaring occurring during any of the observations proposed here are low. Should a flare occur, we will detect it by using the TIME-TAG data to produce light curves of the emission lines, and extract time-resolved spectra to remove the affected times. At the unocculted phases we calculate that we can remove roughly half an orbit of exposure time before the S/N becomes too low to measure the Ly $\alpha$  line with the precision required for this experiment. A flare lasting longer than this would be rare (Froning et al., 2019), and an interesting observation in its own right!

Secondly, the system demonstrates periodic variations caused by the illumination and heating of the side of the Mdwarf facing the white dwarf, which may be a factor when obtaining phase resolved spectra. However, we do not expect this to affect the strength of the emission lines in the ultraviolet. The effect is small at  $\approx 1.5$  percent in the optical bandpass, corresponding to a change in temperature of  $\approx 50 \text{ K}$ . As the emission lines are generated in the stellar atmosphere with formation temperatures of  $10^3 - 10^6 \text{ K}$ , the heating should have no noticeable effect in our observations. Even if this prediction is wrong, by taking zero-velocity observations at both the day and night side (Figure 2), the combined zero-velocity spectra will be an average of the two, equivalent to the maximum velocity phases where half the illuminated side of the Mdwarf is visible. We will be able to monitor for any changes caused by illumination by comparing the fluxes of the other emission lines included in the G140M bandpass, and detecting any change at all would be a novel, unexpected discovery.

## ■ Scheduling Requirements

The target has an ephemeris of  $\text{HJD}=2449800.79131(58)+0.66765930(57)$  (Bleach et al., 2000). We require a single orbit visit at each of phases 0, 0.25, 0.5 and 0.75, with an acceptable phase error of  $\pm 0.05$ . As is standard  $\text{Ly}\alpha$  observations, we require that the observations be obtained such that the Earth's radial velocity relative to the ISM in the direction of the target is small so that the airglow falls into regions where the ISM absorption is deep. Earth radial velocities of  $\pm 20 \text{ km s}^{-1}$  are acceptable, resulting in observing windows of February 09–May 03 and August 09–November 11. Consultation of the APT visit planner shows that there are several weeks–months long visibility windows within those constraints.